

## **Identification and Characterization of Galloping of Tsuruga Test Line Based on Multi-Channel Modal Analysis of Field Data**

**C.B. Gurung<sup>a</sup>, H. Yamaguchi<sup>a,\*</sup> and T. Yukino<sup>b</sup>**

<sup>a</sup> *Department of Civil and Environmental Eng., Saitama Univ., Saitama, Japan*

<sup>b</sup> *Technical Research Center, Kansai Electric Power Co. Inc., Amagasaki, Japan*

Corresponding author: Professor Hiroki Yamaguchi  
Department of Civil and Environmental Engineering  
Saitama University  
255 Shimo-Ohkubo, Saitama 338-8570, Japan

Phone: 81-48-858-3552

Fax: 81-48-858-3552

Email: [hiroki@post.saitama-u.ac.jp](mailto:hiroki@post.saitama-u.ac.jp)

### **Abstract**

In spite of several signal processing and system identification techniques, discussion on field-observed galloping of overhead transmission lines is still based on primitive form of field data such as time series, Lissajous diagrams and power spectra. Any form of large amplitude vibration in ice storms is defined as galloping and an attempt has seldom made in identifying whether such vibrations are self-excited modal responses. In doing so, there are always possibilities of misinterpreting gust response as galloping. In this study, a method of multi-channel modal analysis consisting of Random Decrement Method (RDM) and Eigensystem Realization Algorithm (ERA) is proposed to identify galloping, which is self-excited modal response based on a typical field-monitored data of wind-induced vibration of the Tsuruga Test line. RDM was used to transform the field data into non-forced response component, which is similar to free vibration response, and ERA was used to extract modal parameters from the non-forced components. Based on these modal parameters, galloping events were identified, and characteristics of galloping such as coupled translational and rotational motions, and nature of full span vibration, oscillation envelopes and influence of geometry of the line section to its occurrence are discussed. Result of analysis has confirmed well-known mechanism of bundle conductor galloping, which is galloping of bundle transmission lines involves significant coupling of vertical and torsional motions. As for the characteristics of bundle conductor galloping, the most likely galloping mode in deadend span is found as first asymmetric mode and large amplitude of galloping occurs when torsion is in-phase with vertical velocity. Furthermore, it is found that deadend span line section is more prone to galloping than semi-suspension span line section. Finally, performance of proposed method was tested by introducing usual buffeting analysis, and it is confirmed that it has immense potential to identify and characterize galloping based on field data.

*Keywords:* Transmission line; Field data; Galloping; Gust response; Random decrement method; Eigensystem realization algorithm; Buffeting analysis; Modal analysis; Motion-induced force

## Introduction

Galloping of iced conductors has been a classical design and operating problem since early in last century. Over the decades numerous research programs have been mounted, aimed at identifying the galloping mechanisms [1-6] and preventing galloping or at least minimizing its effects by proposing various devices and techniques [7-10]. In spite of such large-scale studies, several numbers of accidents in transmission lines still keep on happening in ice storms. It is believed that the accidents are due to galloping although actual cause is unknown in majority of the cases. In evaluating such accidents and developing counter measures, it is crucial to have a clear understanding of the nature of vibration that actually occurs in the field. There are, therefore, renewed interests in the field study of galloping of overhead transmission lines.

Purpose of field studies of galloping is normally to improve understanding of the phenomenon. Certain test programs are carried out on spans fitted with artificial ice of some shape in natural wind [11-16]. In such tests, however, question remains regarding how well an artificial ice section represents natural ice, and regarding how broadly the tests with only a few artificial ice shapes can be generalized with respect to variety of natural ice shapes. In order to overcome such shortcomings, there are several tests organized on spans on which natural icing is anticipated [7,17]. The main advantage of testing under natural icing condition is that it is realistic. However, responses observed in such tests are usually somewhat complicated than those observed in span fitted with artificial ice. Therefore, interpretation of such response is difficult and sometimes it may not depend on theoretical assumptions about which even experts may disagree [18]. In spite of this fact, there is usual tendency of paying less attention to discuss galloping based on field data. Any forms of large amplitude vibrations in ice storms are usually defined as galloping and an attempt has seldom made in identifying whether such vibrations are self-excited modal response. In doing so, there are possibilities of misinterpreting gust response as galloping. Presence of large amplitude gust response in transmission lines cannot be overlooked in gusty wind, which has been pointed out by Ohkuma and Marukawa [19].

Since practical engineers are interested mostly on maximum possible peak-to-peak amplitude, discussion on galloping has been based only on primitive data observed in field such as time series, Lissajous diagrams and power spectra. In spite of several signal processing and system identifying techniques, their applications are seldom found in processing of field data of galloping. Recently a study has suggested a method of identifying galloping by analyzing response observed in the field [20]. This study is a step towards using existing signal processing and system identification techniques to discuss galloping observed in the field. The method, however, is based on analysis of single channel response. Therefore, coupling of rotation with translational motion and nature of full span vibration cannot be discussed. These shortcomings can be overcome by employing multi-channel modal analysis, in which coupled torsional and translational responses, and at different locations can be analyzed simultaneously. Since several past studies suggest that galloping of bundle conductors are usually full span modal response, and involves significant vertical, torsional and sometimes even horizontal motion [5, 6, 14-16], use of multi-channel modal analysis is particularly relevant to analyze field data of galloping in bundle transmission lines.

The objectives of this study are to introduce method of appropriate multi-channel modal analysis for identification of galloping based on field data and to discuss characteristics of galloping observed in the Tsuruga Test line. The multi-channel modal analysis used in this study consists of Random Decrement Method (RDM) followed by Eigensystem Realization Algorithm (ERA). RDM is used to eliminate random component of response due to random wind force such that non-forced component of the response can be estimated. From the non-forced components, modal parameters are extracted by ERA analysis, which is applicable to multi-output system and has capability to identify several modal parameters simultaneously.

Based on the extracted modal parameters, galloping is identified, and characteristics of galloping such as galloping mode shape, interaction of translational and rotational motions, oscillation envelopes and influence of geometry of the line section to its occurrence, are discussed. Finally, introducing usual buffeting response analysis performance of the proposed methodology is tested and it is confirmed that the method can identify galloping events correctly based on the field data.

### **Outline of test line and instrumentation**

Kansai Electric Power Company (KEPCO) has been monitoring occurrences of any large amplitude vibrations in Tsuruga Test line during ice storms for past few years [21]. The objective of this field observation is to study galloping of typically large bundle transmission lines in natural wind and icing conditions for different geometries of line sections. The Tsuruga Test line is situated near Tsuruga Bay of Japan, a place with one of typical metrological conditions in winter, which favors occurrence of galloping in transmission lines. Several wind-induced vibration events observed in Phase B and Phase C of the Tsuruga Test line have been investigated in this study. Phase B is two semi-suspension spans line section with four - bundle conductors, while Phase C is two deadend spans with eight and six-bundle conductors (only events in six-bundle conductors are discussed). Top view of the Tsuruga Test lines is shown in Fig. 1, and detail geometrical and natural dynamic characteristics are shown in Tables 1 and 2, respectively [22, 17]. From Table 2, it is apparent that the fundamental mode of Phase C in in-plane motion is two-loops/span mode. It is due to the fact that one-loop/span mode in in-plane motion doesn't exist in deadend span due to required dynamic tension head for this mode [23]. It is noted that one and two-loop/span mode, which is commonly used in galloping of transmission lines, stand for first symmetric and asymmetric mode, respectively.

Measured field quantities are displacement, acceleration, and torsional motion at three different locations along the span (at 1/4, 1/2, and 3/4 points of the span), and wind speed at central tower. Acceleration and torsion were measured by accelerometer and gyroscope, respectively. Although conductor displacements were measured by video picturing of targeted lamps, the displacement response obtained by numerical integration of acceleration is used together with torsional response in the present analysis. It is due to the fact that the displacement response obtained by video picture exhibits several discontinuities because of poor visibility during vibration due to ice storms, which are unsuitable for multi-channel modal analysis.

### **Multi-channel modal analysis for galloping study**

The multi-channel modal analysis used in this study can be divided into two stages, as shown in Fig. 2, where flow chart of multi-channel modal analysis for galloping study is depicted. The first stage consists of RDM, which is used to transform measured response into non-forced component similar to free vibration response. The second stage is extracting modal parameters from data obtained in the first stage analysis. In spite of numerous techniques to extract modal parameters [24-26], ERA [25] is adopted because it is applicable to multi-output systems and has capability to draw several modal parameters simultaneously. Before applying RDM and ERA, preliminary data analysis has been carried out as shown in the steps 1 and 2 of Fig. 2. Firstly, responses measured at several channels, which include vertical, horizontal and torsional responses measured at different locations along the span, are selected for simultaneous multi-channel analysis. Secondly, highpass filter is applied to each response to remove low frequency quasi-static response, which is sometimes dominant in transmission lines as one kind of gust response [20] but unimportant for galloping study. The cut-off frequency for the highpass filter is selected based on the fundamental frequency such that dominant quasi-static response, if any, can be removed effectively without disturbing modal responses.

### *Random Decrement Method*

Random decrement method (RDM) [27-29], which is a method of extracting free vibration component from random response excited by zero mean stationary white noise, is used to extract non-forced vibration by eliminating gust response from measured response of the transmission line. RDM is usually applied in a single response data and level crossing triggering condition, that is, a condition of collecting piece of time series known as random signature at a certain level of displacement, is the most popular triggering condition [28]. In this study, however, horizontal, vertical and torsional responses at three different locations along the span were analyzed simultaneously. Therefore, vertical response at quarter span was selected as reference response and triggering condition was applied to it. With respect to the level crossing triggering condition in reference response, random signatures of selected time lag in all the response channels were collected to yield non-forced response components as shown in the steps 3 and 4 of Fig. 2. By doing so, the phase information among responses at different channel have been maintained, which is necessary to study characteristics of full span and coupled vibrations. It is to be noted that the selection of reference response is justified by the fact that most likely dominant mode in field-monitored vibrations of the Tsuruga Test line is two-loops/span mode, in which vertical response at quarter span is dominant.

### *Eigensystem Realization Algorithm [25]*

Instead of free vibration response as in usual application of system identification, non-forced response components obtained by RDM have been used in the ERA analysis. The Hankel matrix is first formed in the step 5 of Fig. 2 by rearranging the digital data of non-forced components of horizontal, vertical and torsional responses simultaneously so that coupled modal parameters can be identified. The data length of non-forced component, which determines the size of the Hankel matrix, is one of the important parameters in the ERA. That is, some important characteristics of the response cannot be identified if the data length is too short, while modal parameters obtained by considering longer data can be inaccurate as noise to signal ratio is usually high for larger time lag [30]. With several trials and errors, 40 seconds length of non-forced component of the response has been selected in the present analysis.

As shown in the steps 6 and 7 of Fig. 2, the singular value decomposition of the Hankel matrix is next conducted and the model order, which represents double number of dominant modes in the non-forced response, is selected based on relative comparison of the magnitudes of the singular values: The singular value is larger for more dominant mode [31]. The mathematical model is then realized in the state space for the selected model order by deriving the reduced order state matrices of the system and the output, as shown in the step 8 of Fig. 2. The natural frequencies, the modal damping ratios and the complex mode shapes of the dominant modes in the non-forced components of measured responses, are finally determined in the step 9 of Fig. 2 by conducting the complex eigenvalue analysis of the reduced order state matrix of system. It should be noted that the stabilization diagram, which shows a relation between the model order and the identified frequencies of modes, is usually used to check the appropriate selection of the model order as well as the accuracy of identified modal parameters.

### **Galloping identification based on single event**

Out of several field monitored wind-induced vibrations in the Tsuruga Test line an event observed in Phase C is selected and taken as an example to identify whether the event is galloping or not based on multi-channel modal analysis. Vertical, horizontal and torsional responses at three different locations in Fig. 3 (a) were first analyzed by RDM to extract non-

forced components in Fig. 3 (b). As can be seen in Fig. 3 (b), phase information among several responses in a point as well as at different location are maintained by selecting vertical response at 1/4 of the span as a reference response. In this analysis, the triggering level and time lag of random signatures were taken as RMS value of time series and 50 s, respectively. In order to remove quasi-static response component before applying RDM, which is though insignificant for this example problem, a high-pass filter with a cut-off frequency of 0.05 Hz was applied.

The ERA analysis was next performed to identify the model parameters and the result is shown in Fig. 3 (c) as three modal harmonic components simulated by using the identified modal parameters. The model order in ERA was selected as six based on the singular value distribution in Fig. 4, in which three pairs of singular values with relatively larger magnitude are clearly separated from others. The stabilization diagram was also constructed for the model orders form 2 to 20, as depicted in Fig. 5, in order to observe distribution of stable modes and corresponding amplitudes. As can be seen in Fig. 5, there are two closely spaced modes with frequencies close to that of two-loop/span mode. The amplitudes of these two modes are dominant both in vertical and torsional response as shown in Fig. 6, where amplitudes of all the identified modes are plotted with respect to the model order, and the modal parameters of these two modes are tabulated in Table 3. As can be seen in Table 3, Mode I has larger amplitude both in vertical and torsional responses and its damping ratio is lower than the expected structural damping ratio of 0.01-0.02 [32]. This suggests that Mode I can be a galloping with negative aerodynamic damping due to motion-induced force.

The ERA analysis has also confirmed that the shapes of these two modes are two-loop/span in both vertical and torsional motions as shown in Fig. 7. It is to be noted that the mode shape identified by the ERA analysis is a complex one, which exhibits information of both amplitude and phase. Fig. 8 depicts the phase of vertical and torsional modes, which is calculated with respect to vertical response at 1/4 of span. As can be seen in the Fig. 8 (a), the torsional mode in Mode I is leading vertical mode by approximately 90 degree. On the contrary, the vertical mode in Mode II is leading the vertical mode in Mode I by approximately 90 degree and the torsional mode is further leading the vertical mode by 90 degree in Mode II, as shown in Fig. 8 (b). Referring to an expression of energy input to the system by torsion-induced component of the lift in each cycle in Eq. (1), derived by Ratkowski [15], it is apparent that maximum energy is added to the system when torsion ( $\theta$ ) is leading vertical ( $y$ ) by 90 deg, which is the case of  $\theta$  in-phase with vertical velocity ( $\dot{y}$ ), provided that  $C_{L\alpha} > 0$ . Therefore, the condition of phase between vertical and torsional motions in Mode I is such that significant energy can be added to the system by torsional motion.

$$W = qdC_{L\alpha}\theta_{\max}\pi y_{\max} \sin \phi \quad (1)$$

where  $q$  is dynamic pressure head, which is defined as  $\frac{1}{2}\rho U^2$ ,  $\rho$  is mass density of air,  $U$  is mean wind speed,  $d$  is characteristics length of the conductor,  $C_{L\alpha}$  is slope of lift coefficients with respect to angle of attack ( $\alpha$ ),  $\theta_{\max}$  and  $y_{\max}$  are amplitudes of torsion and vertical motion respectively, and  $\phi$  is phase difference between them.

It is concluded here that this event is identified as a coupled galloping because the dominant mode, or Mode I, is full span coupled vibration with negative aerodynamic damping and with conductive phase lag between vertical and torsional motion.

### Some discussion on galloping characteristics

Several characteristics of galloping of bundle transmission lines based on multi-channel modal analysis of field-monitored data in the Tsuruga Test lines are discussed in following sections. Firstly, out of several field-monitored data, most likely series of galloping events were identified by subjective evaluation of non-forced components. It is found that there are three episodes of most likely galloping events in Phase C, which is deadend span but none in Phase B, which is semi-suspension span. The three episodes of most likely galloping events in Phase C are:

- (a) Episode 1: Six events; Jan 08, 1997; Mean wind speed in the range of 10 m/s
- (b) Episode 2: Four events; Feb 22, 1997: Mean wind speed higher than 16m/s
- (c) Episode 3: Six events; Jan 12, 1998: Mean wind speed in the range of 12-15 m/s.

The event, which was discussed in previous section, is one of the events in episode 3.

#### *Modal frequency and damping ratio*

Similarity in each most likely galloping event with the example discussed in previous section is that the displacement response is dominated by two closely spaced modes with frequency close to that of two-loops/span mode. These modes are conductor motion coupled in individual vertical and torsional modes of bundle transmission lines, whose natural frequencies are close to each other. The modal parameters of these two closely spaced modes in the most likely galloping events are shown in Fig. 9, where the dominant mode of Mode I in each event is depicted by filled symbol, whilst the accompanied mode of Mode II by unfilled symbol. All the events in each galloping episode are depicted by the same symbol. In episode 3, the damping ratios of both dominant modes and accompanied modes are very low, as shown in Fig. 9 (b), which are lower than the expected structural damping ratio. Similarly in episode 1, the damping ratio of either dominant modes or that of accompanied modes is smaller than the expected structural damping ratio. Therefore, the events observed in episodes 1 and 3 can be confirmed as galloping events. On the contrary, in episode 2, the damping ratios of dominant modes are clearly higher than the expected structural damping ratio. This means there is occurrence of positive aerodynamic damping in the dominant modes. However, one of the coupled modes in two events is unstable with negative damping. Therefore, these two events out of four events in this episode 2 can also be identified as galloping events. These results have confirmed the well-known galloping mechanism of bundle conductor in the field-monitored data, that is, galloping of bundle conductors occurs due to presence of negative aerodynamic damping of conductor motion either coupled in both individual vertical and torsional mode or one of them.

#### *Mode shape of galloping events*

Based on complex mode shapes obtained in the ERA analysis, amplitude and phase of the complex mode shapes of horizontal, vertical and torsion were calculated and depicted in Figs. 10 (a), (b) and (c), respectively. As can be seen in the figures, the mode shapes of galloping component in all horizontal, vertical and torsional motions are two-loops/span mode regardless of different aerodynamic condition in individual event, which is the fundamental in-plane mode of Phase C. Therefore, the most likely galloping mode in deadend span can be confirmed as first asymmetric mode. Comparison of the mode shapes shows that galloping of bundle transmission lines involves significant vertical and torsional bulk motions, while participation of horizontal motion is relatively less. As for phase difference, the torsional and horizontal modes in episodes 3 are leading vertical mode by slightly less than 90 degree, while they are lagging the vertical mode by slightly more than 90 degree in case of episodes 1 and 2.

### *Amplitude and phase of galloping mode*

In order to study characteristics of bulk motions, amplitudes and phase difference of galloping motions were calculated and are depicted in Figs. 11 (a) and (b), respectively. For the rational comparison of vertical and torsional amplitudes, the torsional amplitude is transformed into equivalent vertical amplitude as follows

$$y_{eq} = r \cdot \tan(\theta) \quad (2)$$

where  $y_{eq}$  is equivalent vertical amplitude,  $r$  is radius of bundle and  $\theta$  twisting angle.

As can be seen from Fig. 11 (a), there is no correlation of amplitude with respect to the mean wind speed. It is due to the fact that amplitude of galloping doesn't depend only on mean wind speed but also on non-linearity in aerodynamic force and other aerodynamic characteristics. In case of episode 3, coupled amplitude of vertical and torsional motions of galloping is comparatively higher than in case of episodes 1 and 2. However, the amplitude fluctuates over a wide range among several events within the episode. Coupling of horizontal motion is relatively weaker as compared to coupling of vertical and torsional motion as shown in the same figure.

Phase difference between vertical ( $y$ ) and torsional ( $\theta$ ) motions of galloping has interesting trend for three different episodes of galloping as shown in Fig. 11 (b). In the events observed during episode 3, the torsional motion is leading vertical motion by approximately 75 degree, which is condition of torsional motion to add energy in its each cycle to the system as is apparent from Eq. (1). It can be one of the reasons to appear large amplitude both in vertical and torsional motions in episode 3 as shown in Fig. 11 (a). In episodes 1 and 2, however, the torsional motion is lagging vertical motion by approximately 110 degree, which cannot be discussed simply based on the simplified Eq. (1). Since the data analyzed in this study is limited, the influence of phase difference between torsion and vertical motion to galloping amplitude has to be studied further.

### *Lissajous diagram*

Lissajous diagrams of representative events in each episode at 1/4 of span are depicted in Fig. 12. Fig. 12 (a) shows Lissajous diagram of galloping component obtained by the modal analysis, in which interaction of horizontal, vertical and torsional motions in terms of both amplitude and phase can be seen clearly. Regardless of different aerodynamic conditions in each event, the oscillation envelope of galloping mode is vertically oriented. As can be seen in Fig. 12 (a), torsional motion involved in episodes 1 and 3 is comparatively higher than in episode 2, which has resulted higher amplitude of galloping component, though the mean wind speed (shown in top-left corner of the Lissajous diagram) in later event is higher than in former events.

The oscillation envelope observed in the field is significantly influenced by presence of gust response. As is apparent in Figs. 12 (a) and (b), Lissajous diagram of representative event of episode 2 in the field is significantly different from that of galloping component. It is due to the fact that there is relatively higher amount of gust response in response to large wind fluctuation as shown in Fig. 13, where RMS of wind fluctuation in three different galloping episodes is shown. Therefore, discussion on galloping based only on field-observed oscillation can sometimes be misleading. Recently, it is suggested that major portion of gust response in transmission lines comes from quasi-static component due to slowly varying wind fluctuation [20]. In such cases, major galloping component can be separated by simply applying high-pass filter with a cut-off frequency close to that of galloping. Fig. 12 (c) shows

Lissajous diagram of major galloping component obtained by high-pass filter. However, it may also contain some higher frequency response. Furthermore, it cannot show how torsional motion interacts with translational motion. It is to be noted that though galloping component obtained by modal analysis consists of single frequency response, there can be contribution of gust at that frequency, which cannot be separated out.

#### *Influence of geometry of line sections*

For the observation period, galloping events are observed only in Phase C, which is deadend span but none in Phase B, which is semi-suspension span. Since both line sections are situated at same location and are subjected to same ice storms, occurrences of galloping only in Phase C indicates that deadend span geometry of the line section is more prone to occurrences of galloping than semi-suspension span. Similar to in-plane motion in deadend span, two-loops/span mode is easily excited than single loop/span mode in torsion. Since the fundamental mode of deadend span in in-plane motion is two-loops/span mode, it is possible that the coupled vertical and torsional motions can readily be excited and become dominant in the presence of large torsional motion. When wind and ice deposits attain conditions where galloping may occur, such dominant mode further increases coherence of aerodynamic force acting on the span to assist occurrence of galloping. Therefore, coupling of large torsional response observed in galloping events as shown in Fig. 14, where RMS of torsion at 1/4 span is shown, can be one of the major causes of galloping in deadend span. Of course, the higher value of torsional motions in Phase B at higher mean wind speed, shown in Fig. 14, has not resulted galloping. It is due to the facts that firstly these torsional motions in Phase B have wide frequency band, which results insignificant coupling at single frequency, and secondly at higher wind speed the chances of occurring galloping is vary rare due to poor coherence of aerodynamic force along the span in high speed gust.

#### **Performance of multi-channel modal analysis to identify galloping**

In order to check the performance of proposed method, RMS of vertical fluctuation observed in the field is compared with corresponding value of expected buffeting response. Figs. 15 (a) and (b) depict RMS of vertical fluctuating component of response measured at field in Phase B and C, and corresponding value of analytically estimated buffeting response at 1/4 span, respectively. The events, which are identified as galloping based on multi-channel modal analysis, are depicted by filled symbols.

The RMS of buffeting response has been analytically calculated by using usual frequency domain method of buffeting analysis. First four modes were considered for modal response synthesis to obtain the buffeting response. Eq. (3) was used to estimate mean square of buffeting response of the  $n^{\text{th}}$  mode [33].

$$\sigma_n^2(q) = \frac{1}{M_n^2 (2\pi f_n)^4} \left\{ \int_0^{f_n} S_{Q_n}(f) df + \frac{\pi f_n S_{Q_n}(f_n)}{4\xi_n} \right\} \quad (3)$$

where  $S_{Q_n}(f)$  is spectrum of aerodynamic modal force, which is defined by  $|J_n(f)|^2 \chi_D^2(f) (\rho_a C_L \bar{U} D)^2 S_u(f)$ ,  $M_n$  is modal mass,  $\xi_n$  is modal damping ratio including aerodynamic damping,  $f_n$  is modal frequency,  $\sigma_n^2$  is mean square,  $C_L$  is lift force coefficient,  $|J_n(f)|^2$  is joint acceptance function, and  $S_u(f)$  is spectrum of longitudinal wind.

From Eq. 3, it is apparent that aerodynamic lift force coefficient, modal damping ratio (sum of structural and aerodynamic damping) and value of wind spectrum are three main parameters, which influenced the buffeting response at a certain mean wind speed. Both aerodynamic damping and aerodynamic lift force coefficients are different for different events observed in the field, which are function of ice shape and wind attack angle, and are usually impossible to generalize by a single value. Therefore, buffeting analysis has been carried out with their expected extreme values; 0.2, 1% and 0.8, 2% are taken as their expected lower and upper values, respectively. Similarly, a lower value of 12% and an upper value of 20% of turbulence intensity, which varies over occasion to occasion, have been selected to estimate the value of wind spectrum. Simiu's longitudinal wind spectrum model [34] was used to calculate the value of wind spectrum, whilst the form of joint acceptance function proposed by Davenport [35] was used to estimate wind force spectrum.

As expected, augmenting action of motion-induced force in galloping response is clearly seen as shown in Fig. 15 (b) with higher value of the galloping response than expected buffeting response. It is particular predominant in the events observed in episode 3 with mean wind speed in the region of 12-15 m/s. Response in these galloping events doesn't follow the trend of the buffeting response, which is parabolic with respect to mean wind speed provided that the aerodynamic damping, turbulence intensity and aerodynamic lift force coefficient remain same. Besides these galloping events, there are few events in Phase C and Phase B with mean wind speed in the region of 10 m/s in which the RMS of response is much higher than the expected buffeting response as shown in the Fig. 15. In these events, however, unlike galloping events the response is mostly constituted by low frequency component indicated by square, which is gust response due to slowly varying wind fluctuation and obtained by evaluating area of power spectra at low frequency range (<0.08 Hz). In other words, the contribution of the modal response, which is difference between total response and background response is very insignificant in these events. It suggests the fact that there is insignificant contribution of aerodynamic motion-induced damping force and hence cannot be galloping i.e. self-excited modal response. Therefore, the performance of proposed multi-channel modal analysis for the identification of galloping based on field-observed data can be regarded as very good. It is to be noted that the curvature of buffeting curve in Phase C, shown in Fig. 15 (b), is shallower than in Phase B, shown in Fig. 15 (a), because the former is stiffer than the later.

## Conclusions

A method of multi-channel modal analysis consisting of RDM and ERA has been proposed to identify galloping, and to discuss characteristics of galloping based on field data. The proposed method is successfully applied to analyze several field-monitored data of the Tsuruga Test line and well-known galloping mechanism of bundle transmission lines is confirmed – conductor motion in galloping events is coupled in individual vertical and torsional natural modes, which are closely spaced in bundle conductors, and galloping occurs when motion coupled at either both modes or one of the modes exhibit negative aerodynamic damping. Furthermore, the performance of proposed method to identify galloping events is tested by carrying out buffeting response analysis, which has shown that the reliability of the method is very good. As for the galloping characteristics of bundle transmission lines based on the field observed data, following major findings are conclusions of this study.

1. Large amplitude of galloping is observed when torsion and vertical motion are approximately in right angle, i.e. case of torsional motion being in-phase with vertical velocity.
2. Most likely galloping mode in deadend span is two-loops/span mode both in vertical and rotational motion.
3. On the contrary to different orientation of Lissajous diagrams observed in field, which is greatly influenced by presence of gust response, the oscillation envelopes of galloping events are vertically oriented.

4. Deadend span is found to be more prone to galloping than semi-suspension span. Application of proposed method to limited data observed in the Tsuruga Test line has shown immense potential to extract parameters from the field data, which have been used to identify and characterize galloping, therefore, the method can be used for this purpose in future.

## References

- [1] J.P. Den Hartog, Transmission line vibration due to sleet, AIEE Transactions 51 (1932) 1074-76.
- [2] O. Nigol, P.G. Buchan, Conductor galloping part I- Den Hartog mechanism, IEEE Transaction on PAS 100(2) (1981) 699-707.
- [3] O. Nigol, P.G. Buchan, Conductor galloping-part II Torsional mechanism, IEEE Transaction on PAS 100(2) (1981) 708-20.
- [4] R.D. Blevins, W.D. Iwan, The galloping response of a tow-degree-of-freedom system, J. Appl. Mech. 41(1974) 1113-18.
- [5] J. Wang, J.L. Lilien, Overhead electric transmission line galloping - A full multi-span 3DOF model, some application and design recommendations, IEEE Transaction on PD 113(3) (1998) 909-16.
- [6] Y. Nakamura, Galloping of bundled power line conductors, J. Sound and Vibration 73(3) (1980) 363-77.
- [7] D.G. Havard, J.C. Pohlman, Field-testing of detuning pendulums for controlling galloping of single and bundle conductors, IEEE Paper A79 (499-5), IEEE symposium on Mechanical Oscillation of Overhead Transmission Lines (1979), Vancouver, Canada.
- [8] J.C.R. Hunt, D.J.W. Richards, Overhead line oscillations and the effect of aerodynamic damper, Proceeding of the IEE, London, 116 (1969) 1869-74.
- [9] A.S. Richardson, Dynamic damper for galloping conductors, Electrical world (1965) 154-155.
- [10] R. Keutgen, J.L. Lilien, A new damper to solve galloping on bundle lines, theoretical background, laboratory and field results, IEEE Transaction on PD 13(1) (1998) 260-65.
- [11] K. Takeda, Introduction of Mogami test line. J. Wind Eng. 65(1995) 51-58.
- [12] G. Diana, F. Cheli, P. Nicolini, F. Tavano, Oscillation of bundle conductors in overhead lines due to turbulent wind. IEEE Transactions on PD 5(4) (1990) 1910-22.
- [13] E.L. Tornquist, C. Becker, Galloping conductors and a method of studying them. AIEE Transactions paper 66(1947) 1154-61.
- [14] A.T. Edwards, A. Madeyski, Progress report on the investigation of galloping, Transaction of AIEE 75 (1956) 666-83.
- [15] J.J. Ratkowski, Experiments with galloping spans. IEEE Transaction on PAS 82 (1963) 661-67
- [16] K. Anjo, S. Yamasaki, Y. Matsubayashi, Y. Nakayama, A. Otsuki, and T. Fujimura, An experimental study of bundle conductor galloping on the Kasatori-Yama Test line of bulk power transmission, CIGRE Report (1974) 22-04.
- [17] T. Yukino, K. Fujii, I. Hayase, Galloping Phenomena of large bundle conductors observed on the full-scale test line, Proceeding of Cable Dynamics, Liege, Belgium (1995) 557-63
- [18] C.B. Rawlins, Transmission lines reference book: Wind-induced conductor motion, Chapter 4 –Galloping conductors, EPRI Research Project 795 (1978) 113-68.
- [19] T. Ohkuma, H. Marukawa, Galloping of overhead transmission lines in gusty wind, First International Conference on Advance in Structural Engineering and Mechanics, Seoul, Korea (1999) 71-76
- [20] C.B. Gurung, H. Yamaguchi, T. Yukino, Identification of large amplitude wind-

- induced vibration of ice-accreted transmission lines based on field observed data, *Eng. Structures* 24 (2002) 179-88.
- [21] T. Yukino, Observation results of galloping phenomenon, *Proceeding of Cable Dynamics*, Tokyo, Japan (1997) 57-62.
  - [22] H. Yamaguchi, X. Xie, T. Yukino, Galloping analysis of transmission lines with bundled conductors, *Proceeding of Cable Dynamics*, Liege, Belgium (1995) 61-6.
  - [23] H.M. Irvine, *Cable structures*, MIT press, Cambridge, Massachusetts (1971).
  - [24] P.V. Overschee, B.D. Moor, *Subspace identification for linear systems. Theory-Implementation-Applications*. Kluwer Academic Publishers, Massachusetts (1996).
  - [25] J. Juang, R.S. Pappa, An Eigensystem Realization Algorithm for modal parameter identification and model reduction, *AIAA, J. Guidance, Control, and Dynamics* 8(4) (1985) 620-27.
  - [26] S.R. Ibrahim, E.C. Mikulcik, A method for the direct identification of vibration parameters from the free response, *Sound and Vibrations Bulletin* (1977) 241-50.
  - [27] A. Kareem, K. Gurley, Damping in structures: its evaluation and treatment of uncertainty, *J. Wind Eng. Ind. Aerodyn.* 59 (1996) 131-57.
  - [28] J.C. Asmussen. Modal analysis based on the random decrement technique- application to civil engineering structures, Ph.D. Thesis, Aalborg University, Denmark (1997).
  - [29] S.R. Ibrahim, Random decrement technique for modal identification of structures, *J. Spacecrafts and Rockets* 14(11) (1977) 696-700.
  - [30] A.P. Jeary, Damping in the structures, *J. Wind Eng. Ind. Aerodyn.* 72 (1997) 345-55.
  - [31] J.M. Caicedo, S.J. Dyke, P. Thomson, J. Marulanda, Monitoring of Bridges to Detect Changes in Structural Health, *Proceedings of the 2001 AACC American Control Conference Arlington, VA* (2001).
  - [32] T. Yukino. T. Kuze, Vibration characteristics in the long span 4 bundled conductors of transmission line, *Proceeding of the Fifth Asia-Pacific Conference on Wind Engineering*, Kyoto, Japan (2001) 193-96.
  - [33] G Solari, Gust excited vibrations, CISM courses and lectures no. 335, International Center for Mechanical Sciences, Springer-Verlag Press, New York (1994) 195-291.
  - [34] E. Simiu, Wind spectra and dynamic along wind response, *J. Struct. Div., ASCE* 100(9) (1974) 1897-1910.
  - [35] A.G. Davenport, Buffeting of suspension bridge by storm winds. *J. Struct. Div., ASCE* 88(3) (1962) 233-68.

## List of Tables

Table 1 Geometric description of the Tsuruga Test Lines [22]

Table 2 Dynamic characteristics of the Tsuruga Test line [17]

Table 3 Modal parameters of dominant closely spaced modes

## List of Figures

Fig. 1 Top view of the Tsuruga Test line, KEPCO

Fig. 2 Flow chart of multi-channel modal analysis for galloping identification

Fig. 3 Schematic diagram of RDM and ERA analysis: (a) Time series of response measured in the field, (b) Non-forced components obtained by RDM and (c) Model components in each non-forced component obtained by ERA

Fig. 4 Singular values distribution of the Hankel matrix

Fig. 5 Stabilization diagram

Fig. 6 Amplitude at 1/4 span of several modes for different model orders: (a) Vertical amplitude and (b) Torsional amplitude

Fig. 7 Amplitude of complex mode shape: (a) Vertical motion and (b) Torsional motion

Fig. 8 Phase of vertical and torsional modes in (a) Mode I and (b) Mode II

Fig. 9 Modal parameters of most likely galloping events: (a) Frequency and (b) Damping ratio

Fig. 10 Amplitude and phase of complex mode shapes of galloping mode: (a) Horizontal motion, (b) Vertical motion and (c) Torsional motion

Fig. 11 Amplitude and phase of galloping mode at 1/4 span: (a) Amplitude and (b) Phase difference of torsion with respect to vertical motion

Fig. 12 Lsajous diagrams of representative events in three different episodes at 1/4 span: (a) Galloping component obtained by modal analysis, (b) Observed in the field and (c) Major galloping component obtained by using high-pass filter

Fig. 13 RMS of wind fluctuation

Fig. 14 RMS of torsional response at 1/4 span

Fig. 15 RMS of vertical fluctuation at 1/4 span: (a) Phase B and (b) Phase C

**Table 1 Geometric descriptions of the Tsuruga Test Lines [22]**

Description	Phase B	Phase C
No. of conductors	4	6/8
No. of spans	2	1
Span length (m)	347 x 2	344
Sag to span ratio	0.037	0.042
Per single conductor		
Unit mass (kg/m/conductor)	3.35	3.35
Axial rigidity (MN/conductor)	65.2	65.2
Conductor diameter (mm)	38.4	30
Conductor spacing (m)	0.50	1.3

**Table 2 Dynamic characteristics of the Tsuruga Test line [17]**

Motion	Mode of vibration (loop/span)	Phase B	Mode of vibration (loop/span)	Phase C
		Natural frequency (Hz)		Natural frequency (Hz)
Horizontal	One loop 	0.14-0.15	One loop 	0.14
	Two loops 	0.28-0.315	Two loops 	0.281
	---	---	Three loops 	0.422
Vertical	One loop (up-down) 	0.166, 0.284	Quasi-one loop 	0.349-0.469
	One loop (up-up) 	0.288-0.320	Two loops 	0.275-0.315
	Two loops 	0.280-0.312	Three loops 	0.470-0.375
Torsion	One loop	--	One loop	0.125-0.148
	Two loop	0.28-0.386	Two loops	0.225-0.297
			Three loops	0.375-0.444

**Table 3 Modal parameters of dominant closely spaced modes**

Mode	Damping (%)	Frequency (Hz)	Amplitude (1/4 span)		Mode shape	Phase between vert. & tors. at 1/4 span (deg)
			Vertical (m)	Torsion (deg)		
I	0.006	0.28	0.503	35.3	Two-loop	79.6
II	0.016	0.27	0.231	18.4	Two-loop	73.00

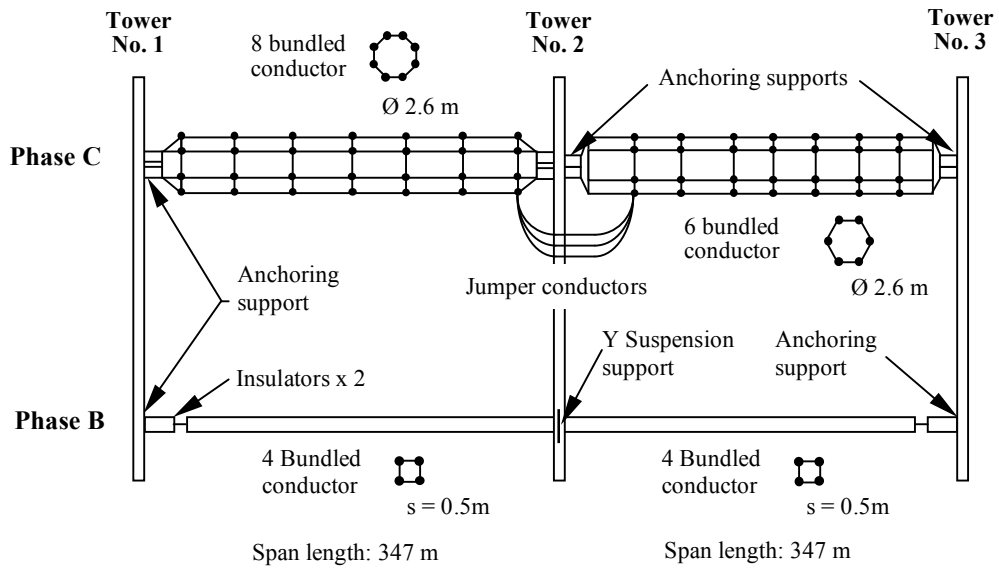


Fig. 2 Top view of the Tsuruga Test line, KEPCO

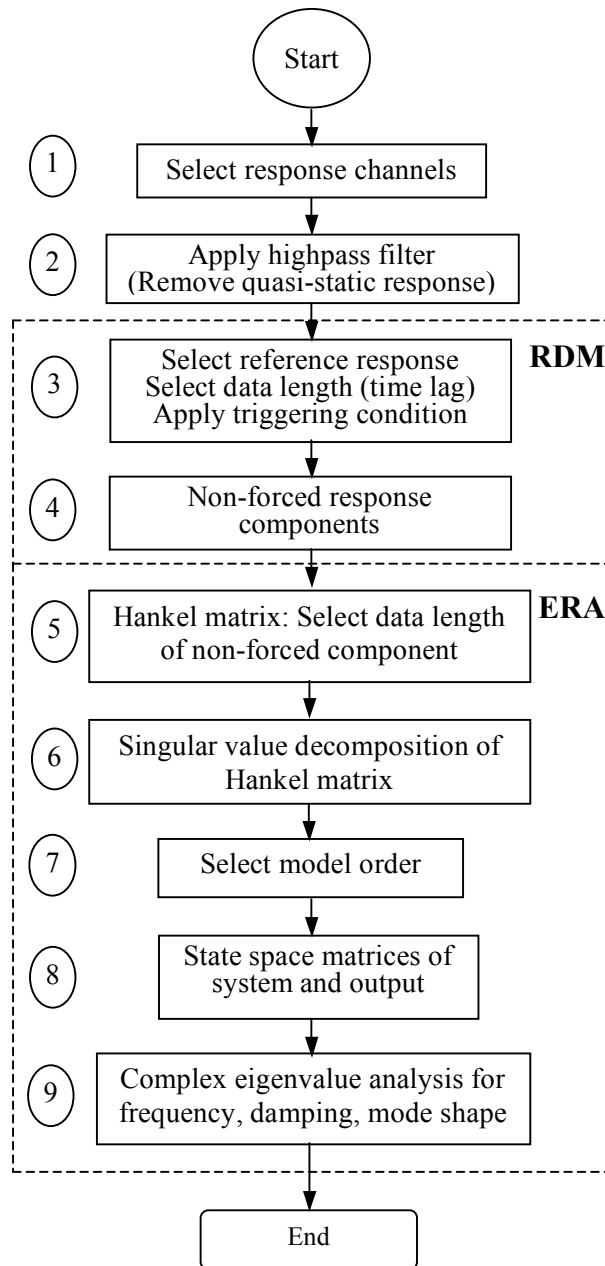


Fig. 2 Flow chart of multi-channel modal analysis for galloping identification

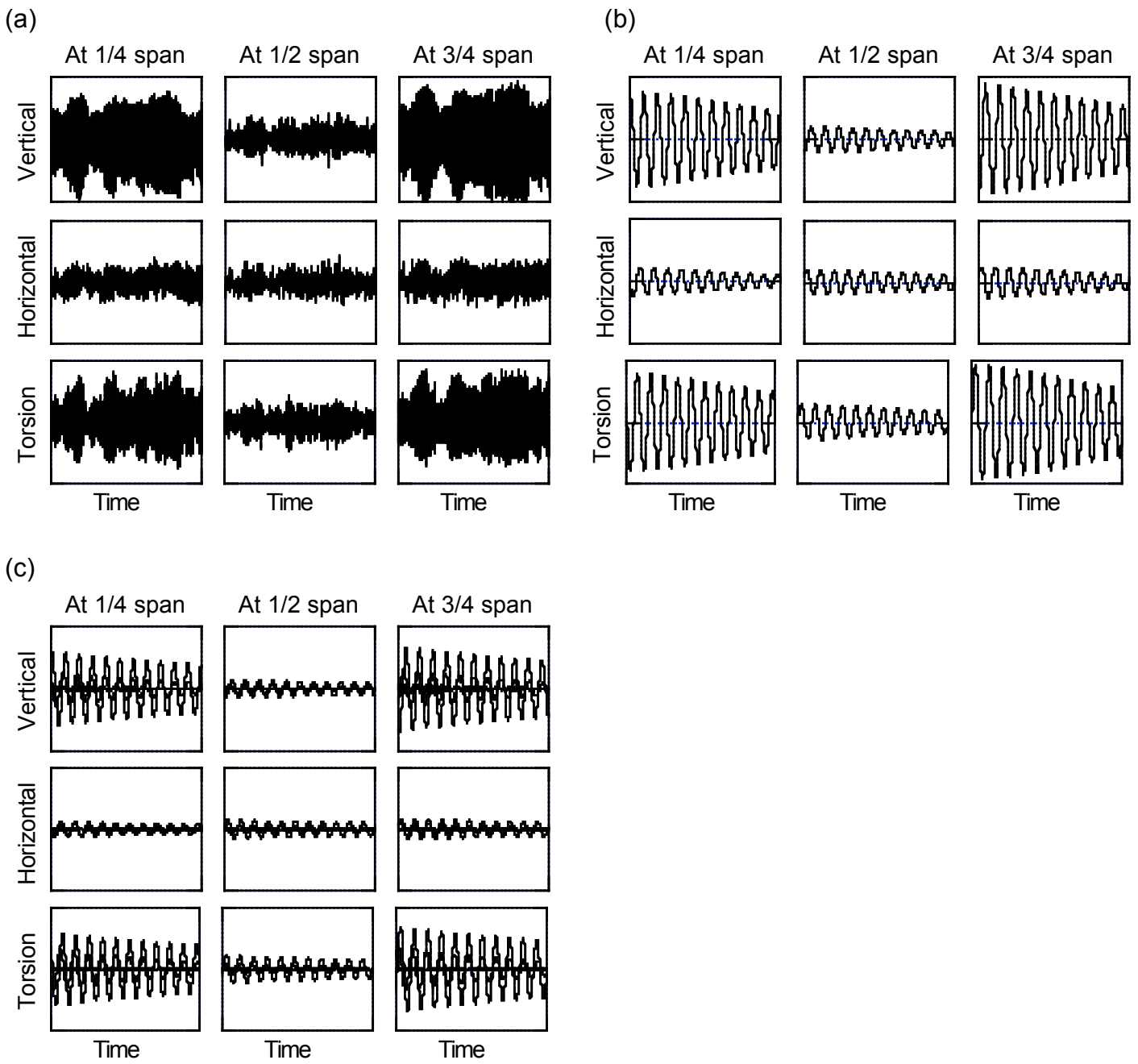


Fig. 3 Schematic diagram of RDM and ERA analysis: (a) Time series of response measured in the field, (b) Non-forced components obtained by RDM and (c) Model components in each non-forced component obtained by ERA

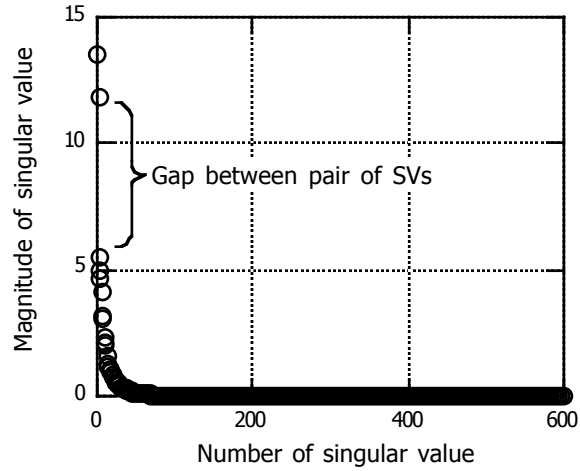


Fig. 4 Singular values distribution of the Hankel matrix

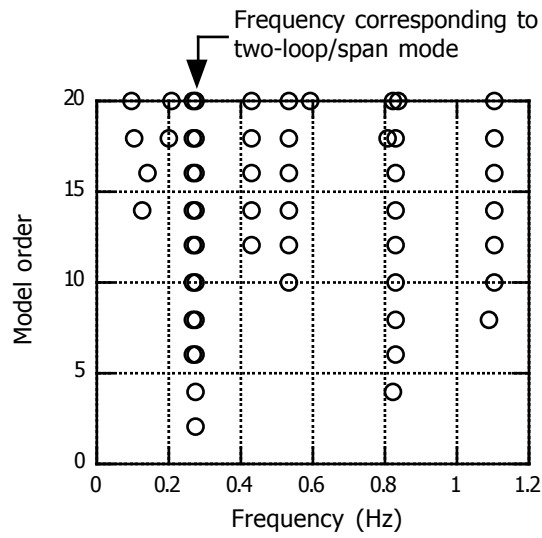


Fig. 5 Stabilization diagram

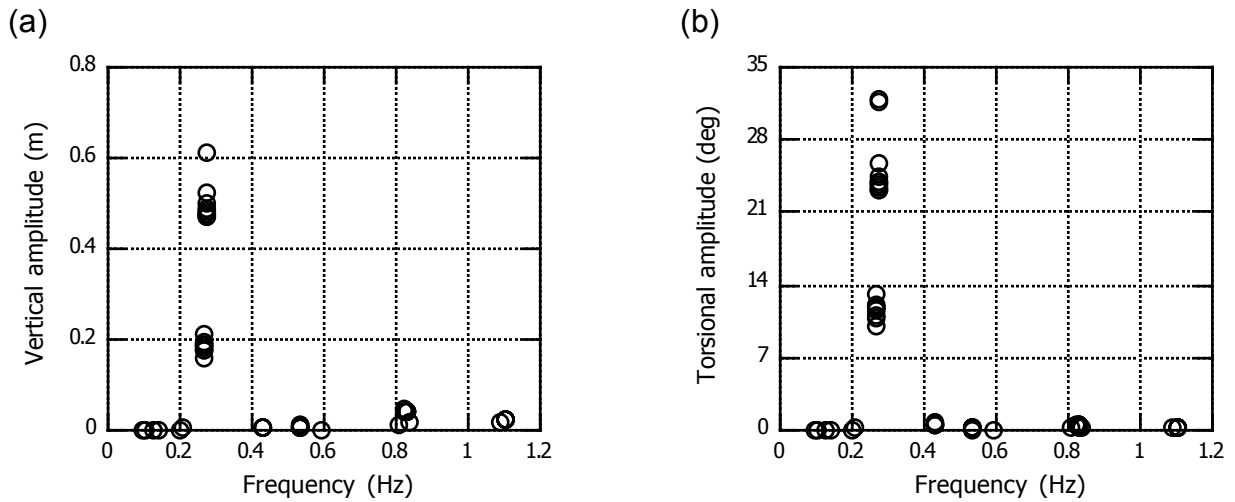


Fig. 6 Amplitude at 1/4 span of several modes for different model orders: (a) Vertical amplitude and (b) Torsional amplitude

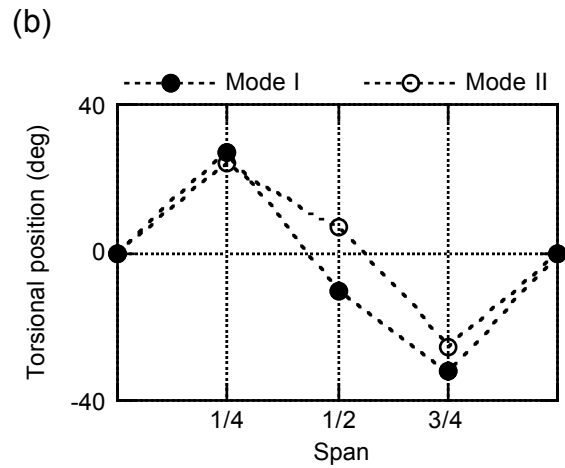
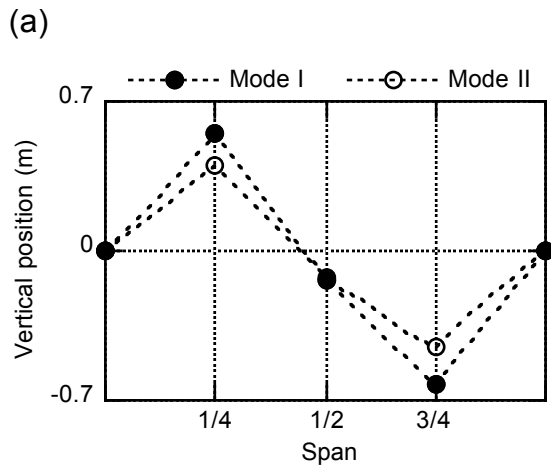


Fig. 7 Amplitude of complex mode shape: (a) Vertical motion and (b) Torsional motion

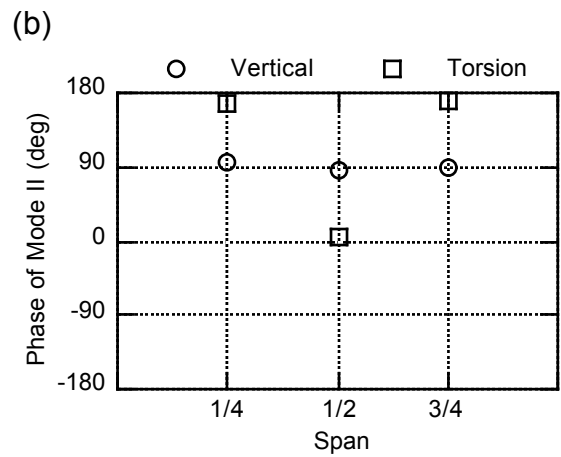
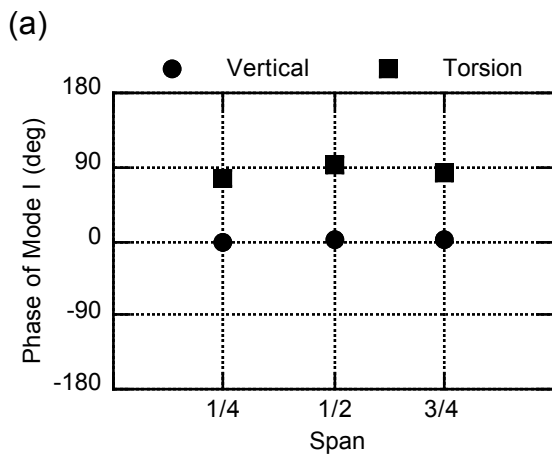


Fig. 8 Phase of vertical and torsional modes in (a) Mode I and (b) Mode II

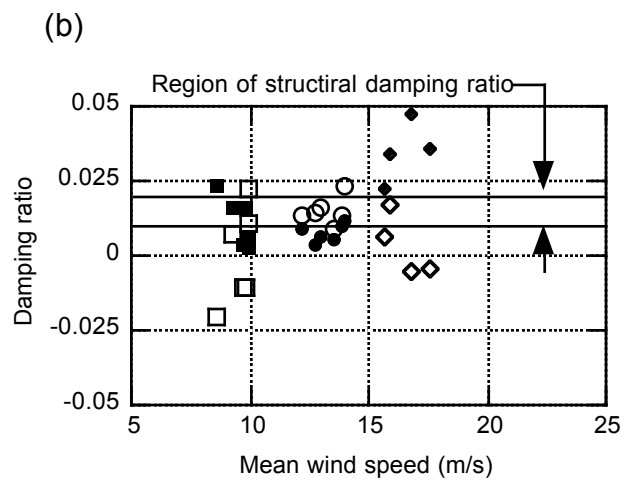
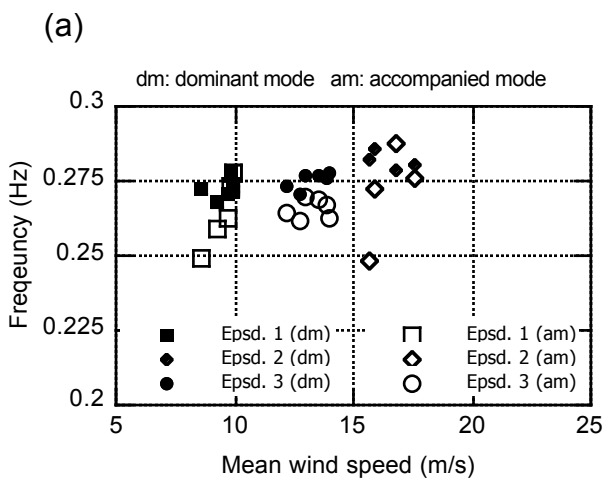


Fig. 9 Modal parameters of most likely galloping events: (a) Frequency and (b) Damping ratio

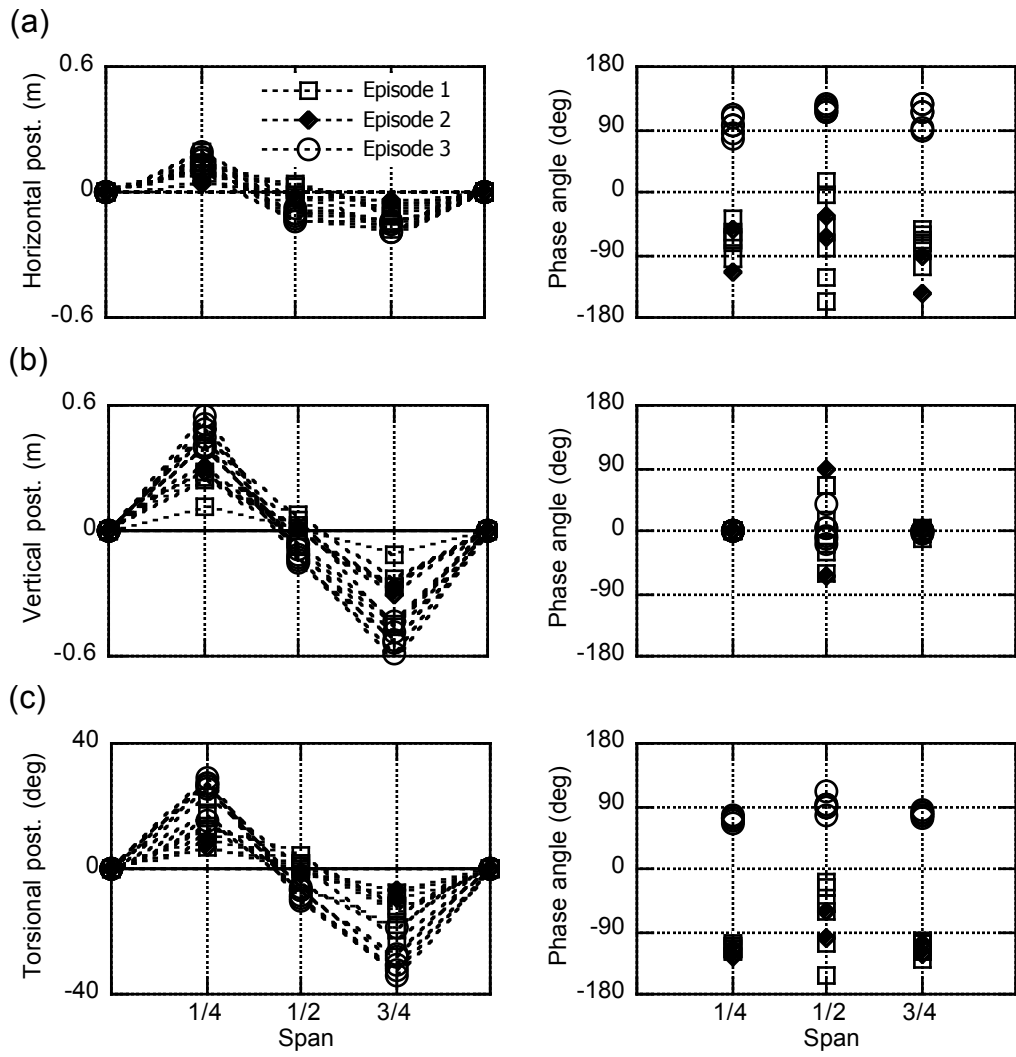


Fig. 10 Amplitude and phase of complex mode shapes of galloping mode: (a) Horizontal motion, (b) Vertical motion and (c) Torsional motion

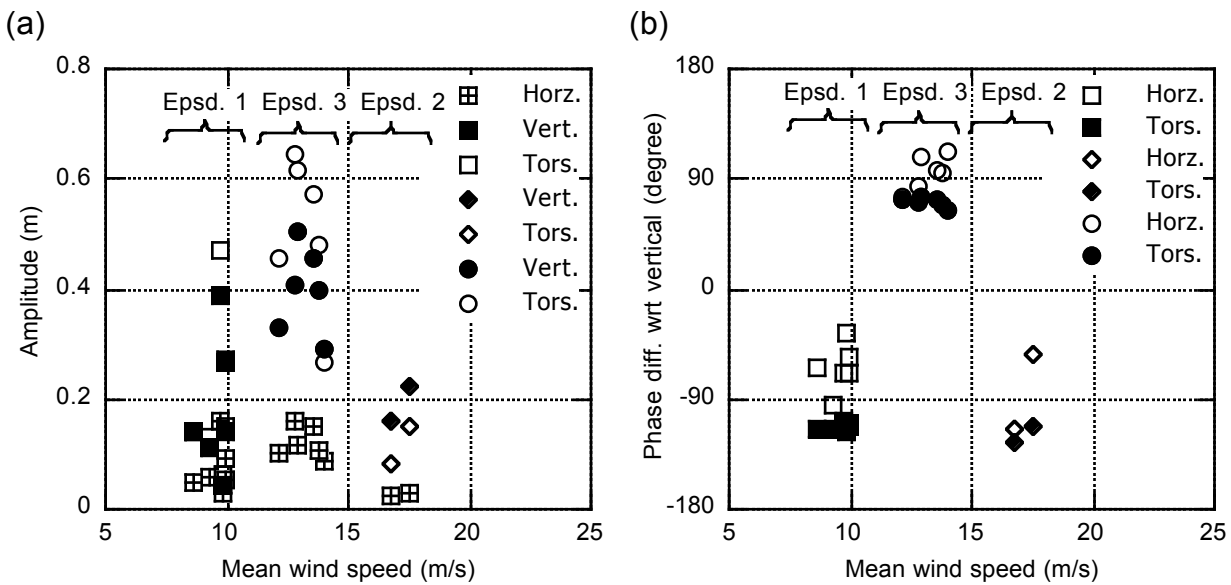


Fig. 11 Amplitude and phase of galloping mode at 1/4 span: (a) Amplitude and (b) Phase difference of torsion with respect to vertical motion

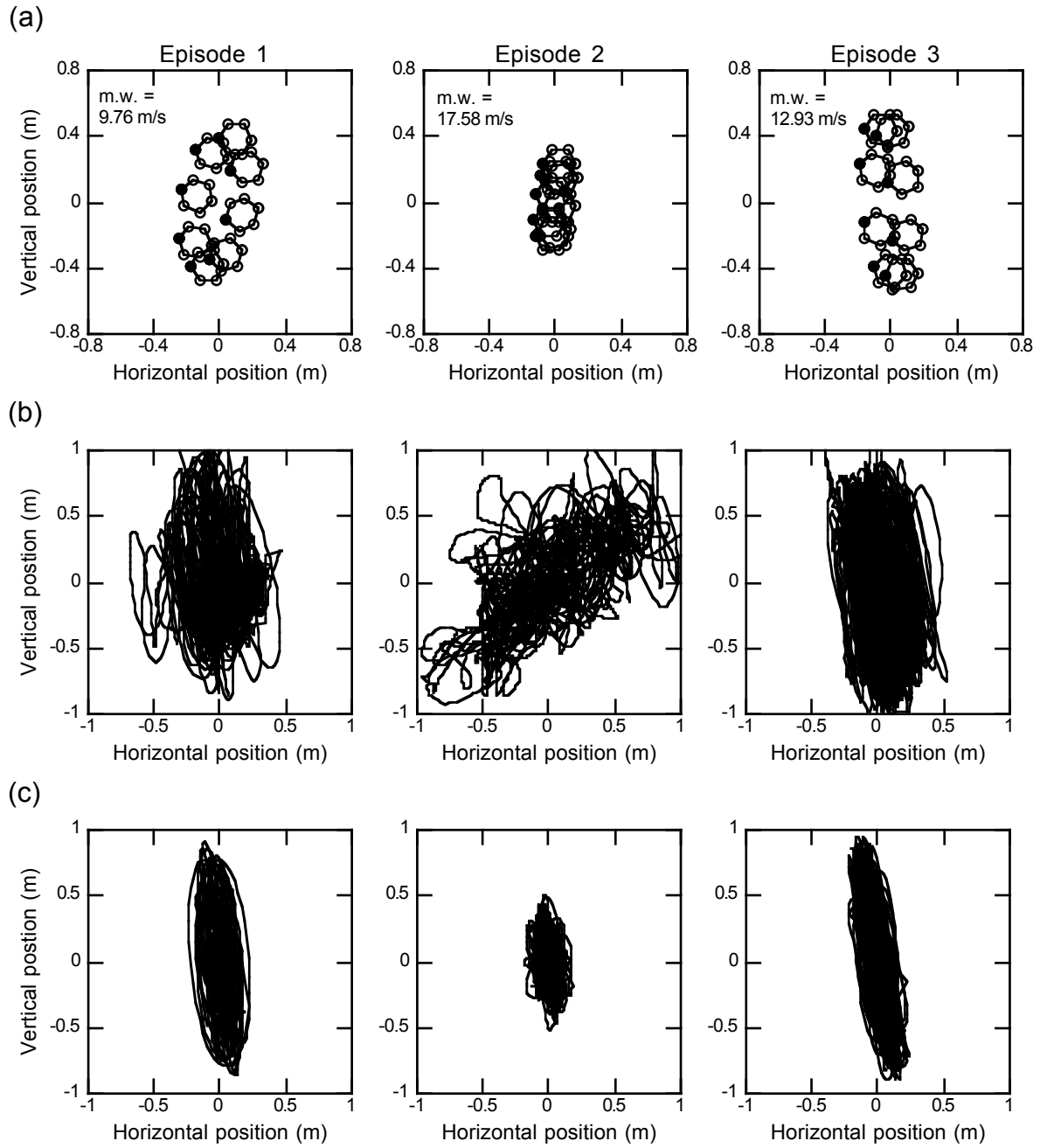


Fig. 12 Lsajous diagrams of representative events in three different episodes at 1/4 span: (a) Galloping component obtained by modal analysis, (b) Observed in the field and (c) Major galloping component obtained by using high-pass filter

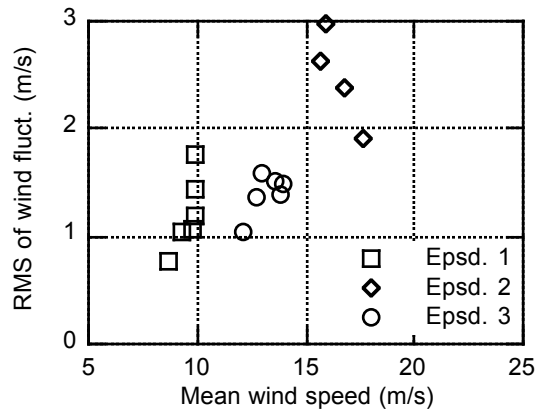


Fig. 13 RMS of wind fluctuation

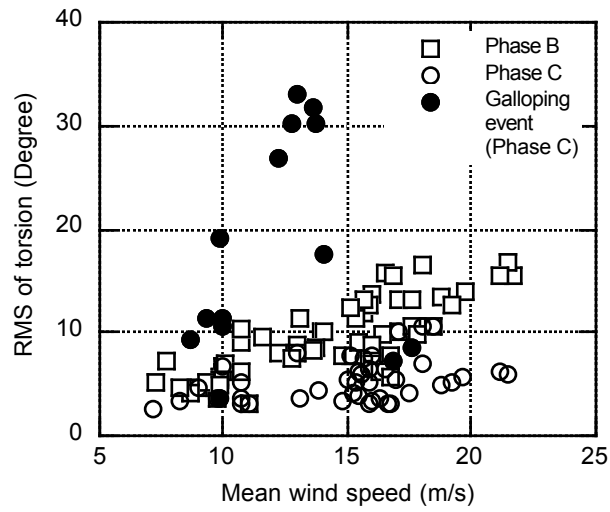


Fig. 14 RMS of torsional response at 1/4 span

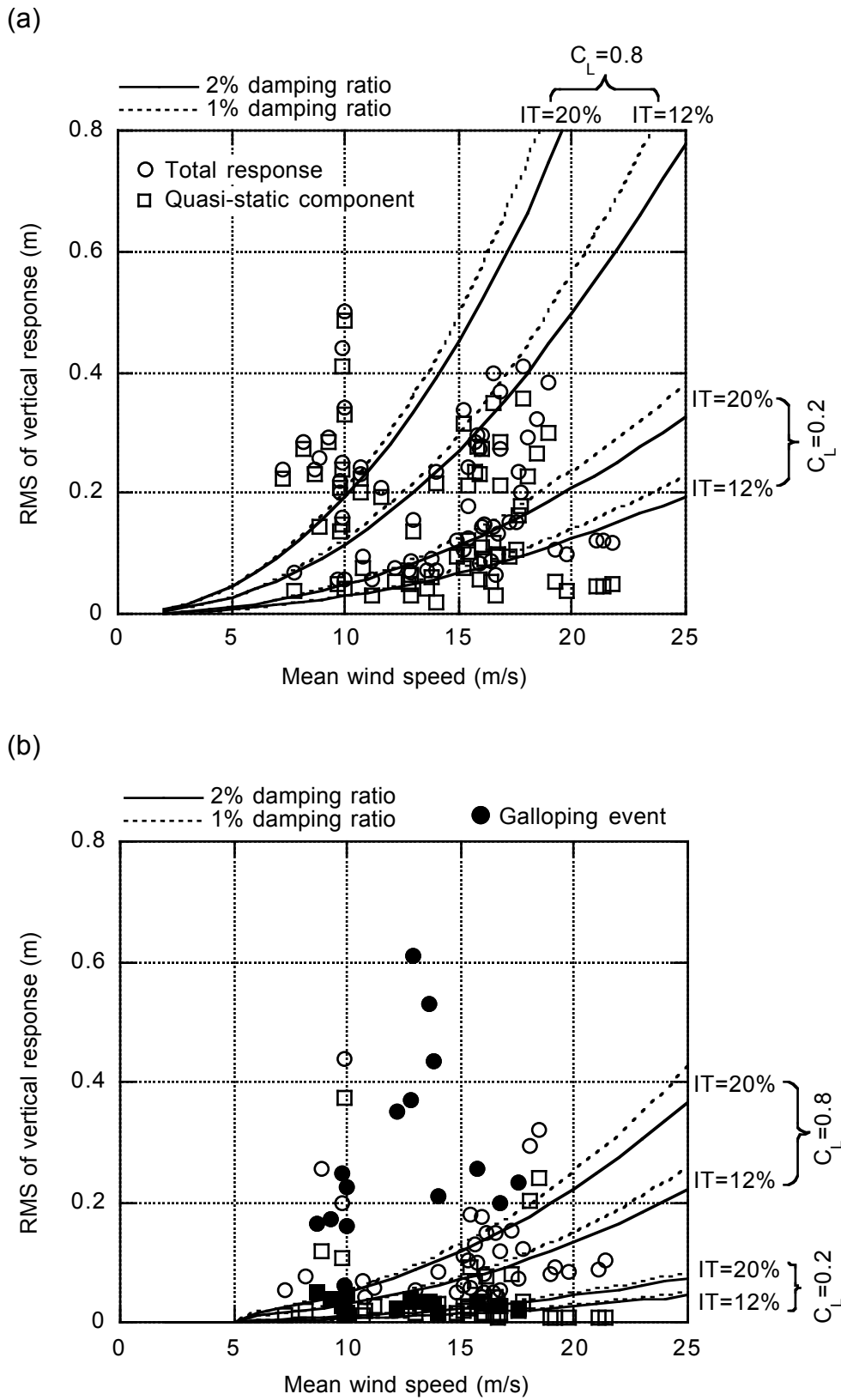


Fig. 15 RMS of vertical fluctuation at 1/4 span: (a) Phase B and (b) Phase C